Nonlinear refraction and optical limiting in thick media

Mansoor Sheik-Bahae
Ali A. Said, MEMBER SPIE
D. J. Hagan, MEMBER SPIE
M. J. Soileau, FELLOW SPIE
Eric W. Van Stryland, MEMBER SPIE
University of Central Florida
Center for Research in Electro-Optics and
  Lasers
Department of Physics and Electrical
  Engineering
Orlando, Florida 32816

Abstract. We experimentally and theoretically investigate optical beam propagation in nonlinear refractive materials having a thickness greater than the depth of focus of the input beam (i.e., internal self-action). A simple model based on the "constant shape approximation" is adequate for analyzing the propagation of laser beams within such media under most conditions. In a tight focus geometry, we find that the position of the sample with respect to the focal plane, z, is an important parameter in the fluence limiting characteristics of the output. The behavior with z allows us to perform a "thick sample Z-scan" from which we can determine the sign and magnitude of the nonlinear refraction index. In CS_2, we have used this method to independently measure the negative thermally induced index change and the positive Kerr nonlinearity with nanosecond and picosecond CO_2 laser pulses, respectively. We have experimentally examined the limiting characteristics of thick CS_2 samples that qualitatively agree with our analysis for both positive and negative nonlinear refraction. This analysis is useful in optimizing the limiting behavior of devices based on self-action.

Subject terms: nonlinear refraction; optical limiting; Z-scan; aberration-free approximation; self-focusing; internal self-action; CS_2.

CONTENTS

1. INTRODUCTION

Passive optical limiters based on nonlinear refraction have been demonstrated and analyzed for a variety of materials and laser wavelengths[1-4] A common geometry is illustrated in Fig. 1. The laser beam is focused into a nonlinear refractive material and is then collected through a finite aperture in the far field. At high irradiance the far field beam distortion arising from the self-action of the laser beam inside the medium will result in the limiting of the transmitted light through the aperture. Most of the published analytical work regarding such a device has dealt with thin samples.[4-6] Here, "thin" means thinner than the depth of focus. Under this thin sample condition, it has been shown[7,8] that the position of the sample with respect to the beam waist (z in Fig. 1) is important in determining the output limiting characteristics. We note that for a thin medium, a displacement of the sample in z by a distance of the order of the depth of focus, can result in reversing the operation of the device from limiting to a transmittance enhancement.[9] We have recently developed a sensitive technique for measuring the sign and magnitude of the nonlinear refractive index n_2 based on the z dependence of the transmitted fluence, which we call a Z-scan.[9,10]

We observe an analogous, but more complicated z dependence for thick limiters (i.e., nonlinear material thickness greater than the depth of focus).[11] It is often desirable to use such thick materials in limiting geometries to either keep the focus away from damage prone surfaces or use in a "self-protecting" geometry.[3,12] Figure 2 shows the energy transmitted through the aperture of Fig. 1 as a function of input energy of 300-ns (FWHM) 10.6-μm pulses using thermal defocusing in CS_2 as the nonlinear mechanism. Plots are shown for three different sample positions relative to the focal plane, showing the sensitivity to sample placement as described above.

Based on a simple "distributed lens" model, we explain the observed limiting behavior of thick limiters as a function of position z. We find that the lowest threshold for limiting is achieved by focusing the beam at the front surface for negative nonlinearity ($\Delta n < 0$) and rear surface for positive nonlinearity ($\Delta n > 0$).

2. MODEL

The nonlinear wave equation governing the propagation of a laser beam inside a nonlinear refractive medium is expressed as

$$\nabla^2 E - \frac{1}{c^2} \frac{\partial^2}{\partial t^2} [(n_0 + \Delta n)^2 E] = 0 , \tag{1}$$

where E is the electric field, n_0 is the linear index of refraction, and the nonlinearity is introduced through Δn, which in general, may include various order contributions such as $\chi^{(3)}$, $\chi^{(5)}$, ... etc. Here, we consider the lowest order effect, namely a $\chi^{(3)}$ (Kerr-type) nonlinearity, which is commonly expressed in terms of the nonlinear refractive index n_2 (esu) as $\Delta n = n_2 |E|^2/2$. In a thick medium, transverse variations accounted for by the ∇^2 term in Eq. (1) become significant and an exact numerical solution to Eq. (1) can be quite complex. A useful technique to
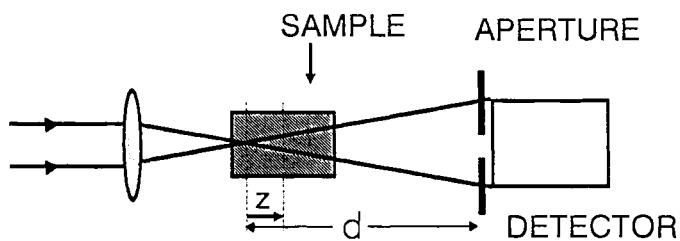
Fig. 1. Schematic of the limiting geometry where z is the distance between the focal plane in free space and the center of the sample, and d is the distance from this plane to the aperture plane.
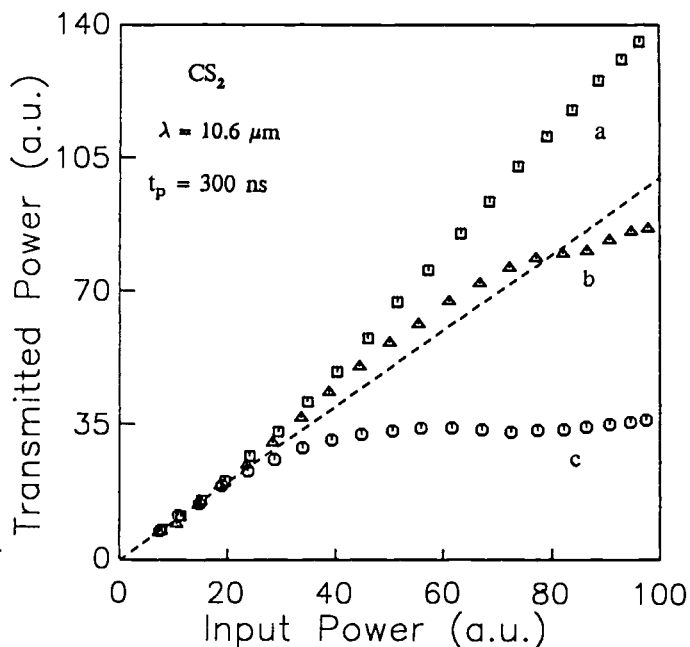

Fig. 2. The limiting characteristics of liquid CS_2 at 10.6 μm measured at various z positions indicated by the arrows in Fig. 9, as explained in Secs. 3 and 4.

simplify this problem is known as the "aberration-free" or "constant shape" approximation,[13,14] in which a Gaussian beam propagating through the thick nonlinear medium is assumed to preserve its Gaussian shape. This requires that the radial variation of the index of refraction be parabolic. For a Gaussian beam and cubic nonlinearity such a requirement is satisfied by using the following approximation:

$$\Delta n(r) = \Delta n(0) \exp(-2r^2/w^2) \simeq \Delta n(0)(1 - 2r^2/aw^2) , \quad (2)$$

where $\Delta n(0)$ is the on-axis index change, w is the local beam radius (HW$1/e^2M$ in irradiance) and we introduce a as a correction factor to account for the higher order terms that have been omitted in the expansion of $\exp(-2r^2/w^2)$. Previous applications of the aberration-free approximation set $a = 1$ (Refs. 13 and 14). Our use of $a \neq 1$ allows for good quantitative agreement in evaluating the nonlinearity or the limiting thresholds. It is expected that the value of a that gives the best fit to the Fresnel wave optics analysis will be geometry and power dependent, and as we will show, a may take on values between 3.77 and 6.4. For a thin medium, the parabolic approximation of Eq. (2) implies that the medium behaves as a thin spherical lens. Therefore, as depicted in Fig. 3, a thick sample can be regarded as a stack of such nonlinear lenses with focal lengths

that depend on the local beam irradiance. The effective focal length of the m'th element in the stack can be written as

$$f_m = \frac{aw_m^2}{4\Delta n_m \Delta L} , \quad (3)$$

where w_m and Δn_m are the beam radius and on-axis index change at that element, respectively. ΔL denotes the separation between two adjacent lenses and should be chosen to be much smaller than both the diffraction length of the beam and f_m. The latter requirement can be written as

$$\Delta L << (aw_m^2/4|\Delta n_m|)^{1/2} . \quad (4)$$

For a given z position of the sample, the input Gaussian beam can be propagated through the nonlinear medium using successive ABCD matrices defined for the m'th element in the stack as

$$\begin{pmatrix} A_m & B_m \\ C_m & D_m \end{pmatrix} = \begin{pmatrix} 1 - \Delta L/n_0 f_m & \Delta L/n_0 \\ -1/f_m & 1 \end{pmatrix} . \quad (5)$$

A final free space propagation ABCD matrix is used to obtain the beam radius at the position of the aperture, w_a, which is now a function of the sample position z and the distance to the aperture. The effect of linear absorption in the numerical calculation can be simply included by replacing Δn_m by $\Delta n_m \exp(-m\alpha\Delta L)$ in Eq. (3).

In the absence of nonlinearity, the field at any position z' is given by

$$E(r,z',t) = E_0(t)\frac{w_0}{w(z')}$$

$$\times \exp\left(-\frac{r^2}{w^2(z')} - \frac{ikr^2}{2R(z')}\right) \exp[-i\phi(z',t)] , \quad (6)$$

where $w^2(z') = w_0^2(1 + z'^2/z_0^2)$ is the beam radius at z', $z_0 = kw_0^2/2$ is the depth of focus of the beam, $k = 2\pi/\lambda$ is the wave vector, λ is the laser wavelength, all in air, and $R(z') = z'(1 + z_0^2/z'^2)$ is the radius of curvature of the wavefront. Here, $\phi(z',t)$ contains all the radially uniform phase terms. The term E_0 denotes the electric field at the focus and contains the temporal envelope of the laser pulse.
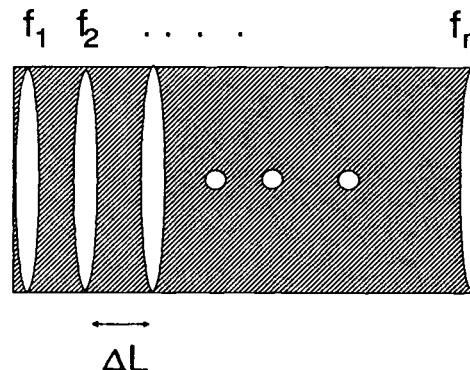

Fig. 3. In the "distributed lens" approximation, the thick nonlinear medium is regarded as a stack of thin nonlinear lenses whose focal lengths depend on the local beam irradiance.

The quantity measured in a limiting experiment or Z-scan experiment is the power P_T (or energy) transmitted through the aperture of radius r_a placed after the sample in the far field. Given the assumption of a Gaussian beam, this quantity, which we write as a function of z, is given by

$$P_T(z) = P_a[1 - \exp(-2r_a^2/w_a^2)] , \tag{7}$$

where P_a is the linear power transmitted to the aperture. Accounting for the temporal variation of a pulse, w_a can be considered a function of time t. The normalized transmittance is then given by

$$T(z) = \frac{\int_{-\infty}^{\infty} P_T(z,t) \, dt}{S \int_{-\infty}^{\infty} P_a(t) \, dt} , \tag{8}$$

where S is the aperture transmittance given by P_T/P_a in the linear (small signal) regime.

We first compare the results for a thin sample using the thin lens approximation to the solution of the wave equation using the Fresnel wave optics approach given in Ref. 10. This allows us to determine the value of the constant a that best approximates the Gaussian beam shape. For the sample at position z with respect to the original focal plane, we can use a single thin lens **ABCD** matrix. With the aperture placed a distance d behind the original focal plane, this leads to the following expression for the spot size w_a;

$$\frac{w_a^2}{w_0^2} = D^2 \left(1 - \frac{2\Delta\Phi_0(D-x)x}{aD(1+x^2)^2}\right)^2 + \left(1 - \frac{2\Delta\Phi_0(D-x)}{a(1+x^2)^2}\right)^2 , \tag{9}$$

where $D = d/z_0$ and $x = z/z_0$. Here, $\Delta\Phi_0$ is the on-axis nonlinear phase shift at focus ($z = 0$), given in terms of the corresponding index change Δn_0 as

$$\Delta\Phi_0 \simeq k\Delta n_0 L , \tag{10}$$

where L is the thickness of the sample. In the case where linear absorption (coefficient α) is present L should be replaced by $[1 - \exp(-\alpha L)]/\alpha$.

Ignoring the temporal dependence, as is appropriate for a steady state condition, and using Eqs. 7 and 8 we obtain

$$T(z) = \frac{1 - \exp(-2r_a^2/w_a^2)}{S} . \tag{11}$$

For a thin sample in the geometry of Fig. 1, the transmittance calculated using the Fresnel wave optics approach as a function of sample position for a fixed input irradiance is shown in Fig. 4 along with the results obtained from Eq. (11).[10] In these calculations a positive nonlinearity with a $\Delta\Phi_0$ of 0.5 rad was assumed. As shown in Fig. 4, the agreement in the total transmission change (from the valley to the peak) is quite good choosing $a = 5$ for $S = 0.5$. In general, based on a detailed numerical analysis, we find that the peak to valley transmittance change is fit to within $\pm 5\%$ accuracy by choosing a as given by

$$a \simeq 6.4(1 - S)^{0.35} \quad \text{for } 0 \leq S \leq 0.7 \text{ and } \Delta\Phi_0 \leq \pi/2 . \tag{12}$$

Numerical analyses show that at larger phase distortions a will decrease further. For very large induced phase distortions in thick materials we choose $a = 3.77$ for reasons explained in Sec. 4. The low-field small-aperture ($S \simeq 0$) limit of this relation ($a = 6.4$) can be easily derived from Eq. (9) as shown in the Appendix. The deviation of a from Eq. (12) at higher irradiance reflects deviations from the constant shape approximation at large phase distortions.

3. Z-SCAN

Plotting the z dependence of the transmittance as shown in Fig. 4 is a sensitive and useful way to characterize the limiting properties of the nonlinear material. Such pronounced variations of the beam transmittance through the aperture as a function of the sample position z have also provided the basis for an extremely simple and sensitive technique that we call Z-scan and use for accurate measurements of refractive nonlinearities.[9,10]

The Z-scan technique is based on the transformation of phase distortions to amplitude distortions during beam propagation. The Z-scan experimental apparatus is as shown in Fig. 1, where the sample is moved along the propagation direction z while keeping the input pulse energy fixed. A qualitative physical argument that explains the transmittance variations in the Z-scan experiment[10] can be given as follows: Starting the scan from a distance far away from the focus (negative z), the beam irradiance is low and negligible nonlinear refraction occurs leading to linear transmittance. We normalize the linear transmittance to unity. As the sample is brought closer to the focus, the beam irradiance increases leading to self-lensing in the sample. A negative self-lensing prior to focus tends to collimate the beam and reduce the diffraction leading to a smaller beam at the aperture and an increased transmittance. As the scan continues and the sample crosses the focal plane to the right (positive z),
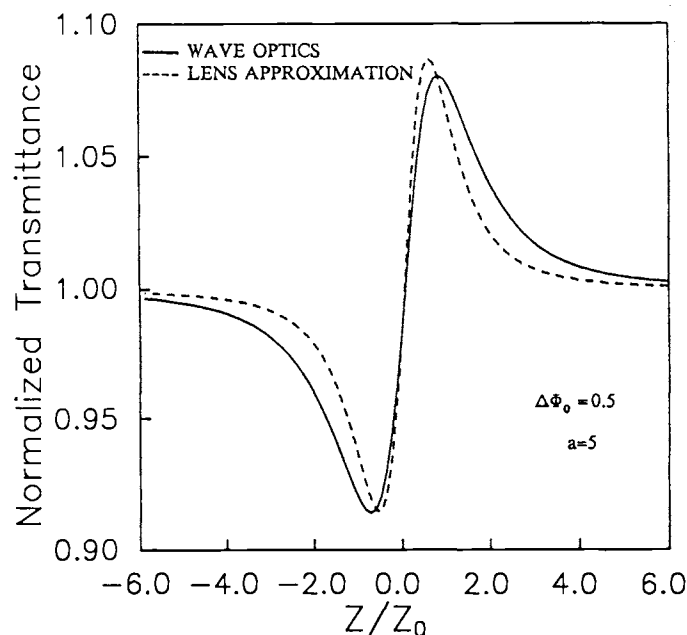

Fig. 4. The Z-scans of a thin nonlinear medium as calculated using the methods of wave optics (solid line) and the thin lens approximation (dashed line). A 50% aperture is assumed ($S = 0.5$).

the same self-defocusing effect will tend to augment diffraction and reduce the aperture transmittance. A prefocal transmittance maximum (peak) and a postfocal transmittance minimum (valley) are, therefore, the Z-scan signature of a negative nonlinearity, while a positive one, following the same analogy, will give rise to an opposite valley-peak configuration. With a small phase shift and a thin sample, the peak and valley are[9,10] symmetrically positioned about the focal plane and are separated by a distance $\Delta Z_{p-v} \simeq 1.7z_0$. This separation is given by the wave optics calculation, while the constant shape approximation gives a somewhat smaller value, as described in the Appendix.

We have used such thin sample Z-scan data to measure n_2 of a large class of materials with a demonstrated sensitivity of $\simeq \lambda/300$ wavefront distortion.[10] Here we extend the applicability of the Z-scan method to thick samples. With a limiting device in mind, the obvious optimum sample position to minimize the limiting threshold is the z region where the valley occurs. We will exploit this feature further in optimization of thick limiters.

The calculated Z-scan for a rather extreme case in which $L/(n_0 z_0) = 15$ is shown in Fig. 5. For a thick sample, z is defined as the distance from the center of the sample to the position of the focus in air in the absence of the nonlinear medium. A cubic nonlinearity with either sign and with $\Theta/a = \pm 0.5$ is assumed where $\Theta = k n_0 \Delta n_0 2z_0$. Note that Θ is approximately the induced phase distortion accumulated in the sample between $-z_0$ to $+z_0$. An interesting feature of the thick sample Z-scan is that the separation between peak and valley of these curves is now dominated by the optical length of the sample, L/n_0. Furthermore, the two extremes correspond to focusing the laser beam on either surface. More generally, we find $\Delta Z_{p-v}(\text{thick}) \simeq [(L/n_0)^2 + \Delta Z_{p-v}^2(\text{thin})]^{1/2}$ where $\Delta Z_{p-v}(\text{thin})$ is the thin sample limit of $\simeq 1.7z_0$. Also evident from Fig. 5 is the existence of a nearly flat transmittance region where the beam is focused near the middle of the medium. This simply signifies the fact that although the laser beam experiences a large local phase distortion within the medium, the effects of prefocal and postfocal nonlinear refraction are nearly cancelled in the far field. Using the lens analogy, the effect is similar to placing a pair of lenses of

the same sign on both sides of the focal plane such that the far field beam pattern is relatively unaltered.

The observations reported in the "Chinese Tea" paper[15] are easily understood from the above analysis. In that paper, they observed a beam narrowing and expansion depending on the position of the focus within the linearly absorbing sample. This was interpreted as a change in sign of the nonlinearity. Clearly, for a purely defocusing nonlinearity both beam expansion and beam narrowing can be obtained in a thick sample depending on the position of the focus within the sample. We, therefore, explain their results as being due to simple thermal defocusing caused by linear absorptive heating.

The existence of a large internal self-action results in a larger transmittance change for a positive nonlinearity than for a negative one of the same magnitude as seen in Fig. 5. This results from the fact that with a positive nonlinear index the resultant self-focusing is a self-strengthening effect similar to an avalanche process, whereas with a negative nonlinearity we have self-defocusing inside the medium, which leads to a self-weakening of the nonlinear refraction. Nevertheless, at small enough phase distortions where variations of the beam diameter inside the medium due to nonlinear refraction are insignificant, nonlinearities with opposite signs will give rise to the same peak to valley transmittance changes.

It is useful to look at what we call the effective interaction length inside the nonlinear material. Clearly for samples much thicker than z_0, making the sample thicker will no longer increase the total ΔT_{p-v}. We define L_{eff} as

$$L_{eff} = \frac{\Delta T_{p-v}(\text{thick})}{\Delta T_{p-v}(\text{thin})} L , \qquad (13)$$

where $\Delta T_{p-v}(\text{thick})$ is calculated using the distributed lens method and $\Delta T_{p-v}(\text{thin})$ is calculated assuming that the sample is much thinner than the depth of focus. As reported in Ref. 10, $\Delta T_{p-v}(\text{thin})$ is given by

$$\Delta T_{p-v}(\text{thin}) \simeq 0.406(1 - S)^{0.25}\Delta\Phi_0 \qquad (14)$$

with $\Delta\Phi_0$ defined by Eq.(10).

To graph the results in a way that will be useful in extracting the total phase distortion in the thick sample, we define the dimensionless parameters $l_{eff} = L_{eff}/n_0 z_0$, and $l = L/n_0 z_0$. Figure 6 shows l_{eff} for various values of Θ/a as a function of l. Figure 6 also shows how defocusing ($\Theta < 0$) lowers l_{eff} and self-focusing ($\Theta > 0$) raises l_{eff} as the beam size within the thick ($l > 2$) material is broadened ($\Theta < 0$) and narrowed ($\Theta > 0$), respectively. The curves in Fig. 6 were calculated using $S = 0.5$. Further calculations have shown that l_{eff} is highly insensitive to S.

We see, as expected, that $l \simeq l_{eff}$ for small l and that most of the total phase distortion or index change is achieved within a sample of thickness $\simeq 2z_0$. Further increases in the sample length lead to only small increases in the Z-scan signal (ΔT_{p-v}) and in the same way will be less effective in lowering a limiting threshold. Applications exist(e.g., when linear absorption is present) where we wish to maximize the phase distortion with a minimum of sample length or linear loss.

As given in Fig. 6, l_{eff} also can be used to obtain an accurate estimate of the induced phase change Θ and, thus, the nonlinear refractive index of the sample. This can be achieved by noting that combining Eqs. (13) and (14) yields
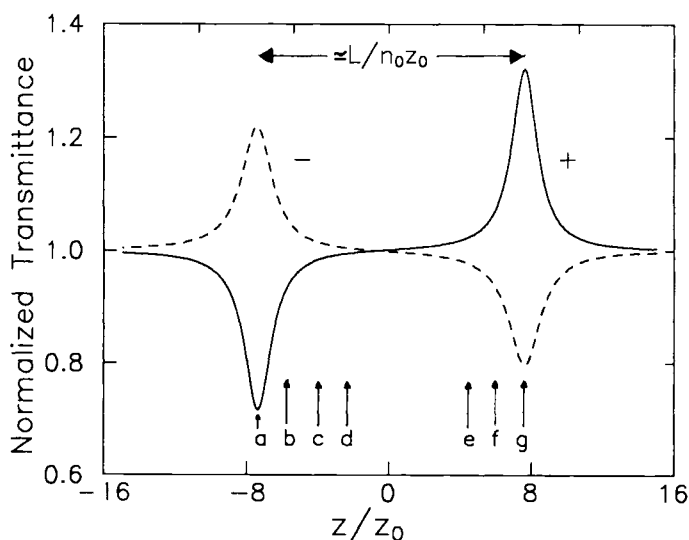

Fig. 5. Calculated Z-scans of a thick medium using the distributed lens method for both positive (solid line) and negative (broken line) nonlinearities ($\Theta/a = \pm 0.5$). The arrows on the z-axis indicate the corresponding positions at which the limiting curves of Figs. 7 and 8 were obtained (see Sec. 4). Here, we chose $n_0 = 1$ and $S = 0.5$.
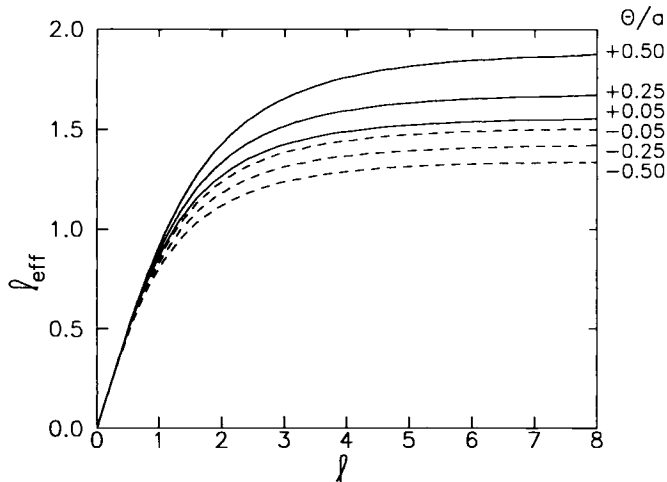
Fig. 6. Calculated effective interaction length as a function of the sample length in units of z_0 for various degrees of nonlinear phase distortion Θ/a.

$$\Delta T_{p-v}(\text{thick}) \simeq 0.406(1 - S)^{0.25} \frac{\Theta l_{eff}}{2} . \quad (15)$$

Here $\Theta l_{eff}/2$ can be interpreted as the effective on-axis nonlinear phase shift when the focus is at the center of the sample. Because, according to Fig. 6, knowing l_{eff} requires knowledge of the value of Θ, an iterative procedure can be used that converges rapidly to give Θ and, thus, Δn_0. One may start by assuming a small $|\Theta|$ (≤ 0.2). Using Fig. 6, given this Θ and l, we obtain an l_{eff}. Using this l_{eff}, a new Θ can be reevaluated from Eq. (15). Repeating the process quickly converges to the correct Θ. Although the curves in Fig. 6 were obtained assuming a lossless medium ($\alpha = 0$), the same curves can be used if linear absorption is present, provided that the left-hand side of Eq. (15) is multiplied by the absorption factor $[1 - (\exp - \alpha L)]/(\alpha L)$. Numerical calculations show that this procedure works well for $\alpha L < 2$ as long as $|\Theta| < 2$.

4. LIMITING

As for the case of a thin sample, to maximize the limiting effect, we must place the thick sample at a position where the transmittance shows a valley similar to the one in Fig. 5. The theoretical limiting behavior of the thick medium of Fig. 1 is shown in Figs. 7 and 8 for negative and positive nonlinearities, respectively. As the sample is positioned farther from the valley, the limiting threshold increases. We define the limiting threshold as the input at which the transmittance drops by a factor of two. For negative nonlinearity, the lowest limiting threshold is obtained at the valley corresponding to focusing at the front surface. This threshold is given by $\Theta \simeq a$. Focusing near the rear surface yields a transmission enhancing behavior that is undesirable for a limiting device. Similarly, for a positive nonlinearity, the lowest limiting threshold occurs at the valley that corresponds to rear surface focusing. However, as seen in Fig. 8, a sudden drop of transmission occurs at $\Theta \simeq a$ due to the onset of catastrophic self-focusing. This threshold is seen to be nearly independent of the sample position. The term Θ can also be expressed as a power ratio:P/P_1, where P denotes the radiation power and P_1 is defined as the first critical power for self-focusing[16,17]:
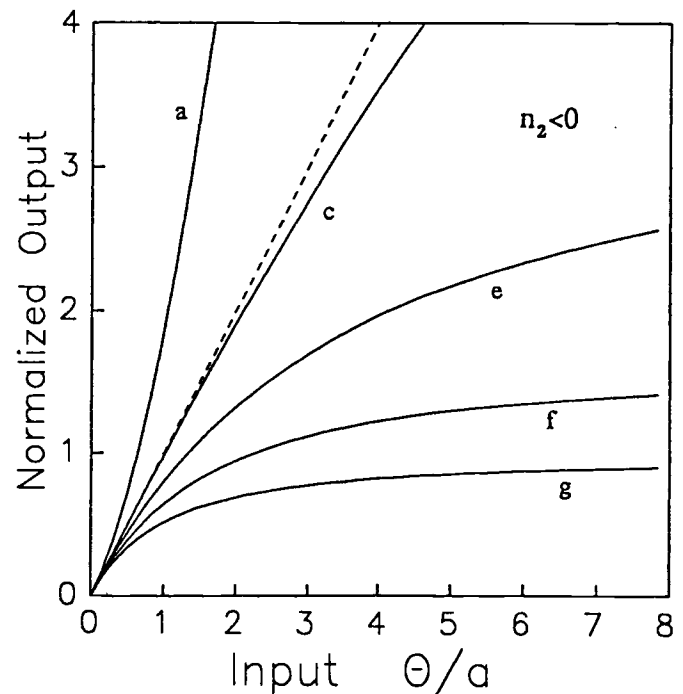

Fig. 7. The normalized limiting curves for a negative nonlinearity ($n_2 < 0$) calculated for various sample positions (z) as indicated by the arrows in Fig. 5. The broken line shows the linear transmittance. ($S = 0.5$ was used in the calculations).
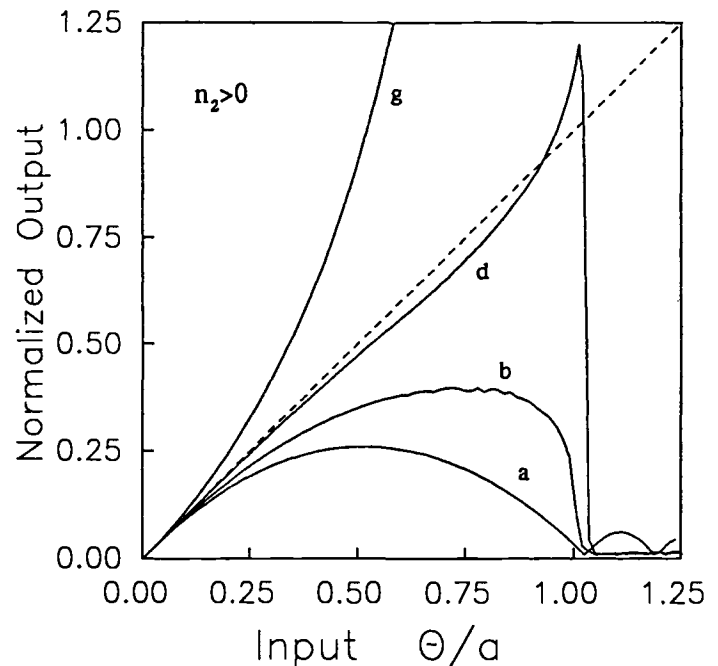

Fig. 8. The normalized limiting curves for a positive nonlinearity ($n_2 > 0$) calculated for various sample positions (z) as indicated by the arrows in Fig. 5. The broken line is the linear transmittance curve. Catastrophic self focusing occurs in all the curves at $\Theta/a \simeq 1$ signified by a sudden drop in the transmitted power. ($S = 0.5$ was used in the calculations).

$$P_1 = \frac{c\lambda^2}{32\pi^2 n_2} \quad \text{(cgs units)} . \quad (16)$$

Numerical calculations of the nonlinear wave equation made by Marburger[18] indicate that for focused Gaussian beams in a thick

medium with positive nonlinear index($n_2 > 0$), a catastrophic self-focus will occur at a critical power of $P_c = 3.77 P_1$ ($\Theta = 3.77$). The distributed lens method, therefore, predicts the correct result, choosing $a = 3.77$, as stated in Sec. 2 for large induced phase distortion.

Referring to Fig. 8, when the self-focusing threshold is reached, the laser beam is predicted to collapse and the local beam irradiance to become infinite. However, the paraxial approximation and, hence, the analysis breaks down as the beam radius becomes[19] comparable to the wavelength λ. In addition, at the high irradiance produced by the self-focusing effect, one must consider higher order nonlinearities as well as plasma production and subsequent optical breakdown of the medium.

5. EXPERIMENTS

Optical limiting in liquid CS_2 was examined using a TEA CO_2 laser with single longitudinal mode pulses of 300-ns duration. The laser beam was focused to $w_0 \simeq 60$ μm ($z_0 \simeq 1$mm) into a 24-mm cell (with NaCl windows) filled with spectrophotometric grade CS_2. With $n_0 = 1.63$, the ratio $L/nz_0 \simeq 15$, indicating a thick medium. First, we performed a Z-scan on this sample to verify the locations of the peak and valley of the transmittance. The result for a 1-mJ pulse energy along with the theoretical fit is shown in Fig. 9. The curve exhibits features predicted by the distributed lens method for a negative nonlinearity, namely the peak and valley corresponding to the second and first surface focusing, respectively, and a nearly flat portion corresponding to focusing near the center of the cell. The origin of this negative nonlinearity is believed to be thermal, arising from the finite absorption of 10.6-μm radiation in CS_2 ($\alpha \simeq 0.22$ cm^{-1}). Thermal lensing in liquids arises from the thermal expansion of the medium and has a rise time given by the "acoustic transit time," which is effectively the time a sound wave takes to traverse the beam radius.[20] Knowing the sound velocity in CS_2 ($v_s \simeq 1.5 \times 10^5$ cm/s) and the focal beam radius ($\simeq 60$ μm), a response time of $\simeq 40$ ns is obtained, which is almost an order of magnitude smaller than the laser pulsewidth. The decay of the thermal lens, however, is governed by the thermal
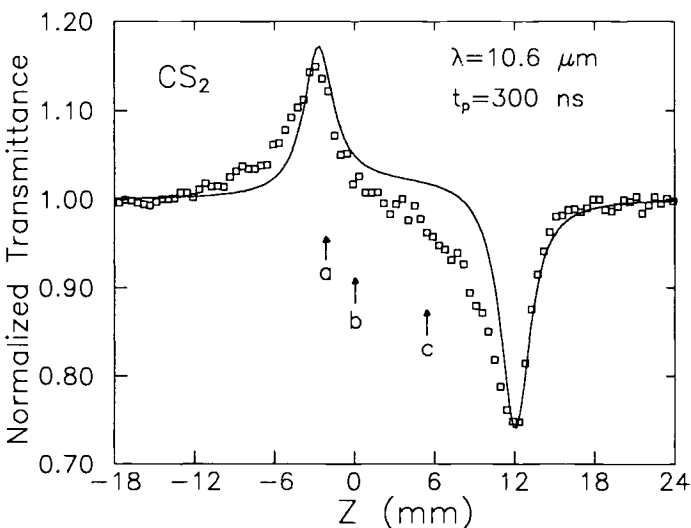
diffusion process, which is on the order of 0.1 s, which is orders of magnitude larger than the pulsewidth and can be neglected.[20] Under such quasi-steady state conditions, the time averaged nonlinear index change ($\langle \Delta n_0 \rangle$) arising from nonuniform heating can be estimated in terms of the laser pulse fluence (F) at the focus[10]

$$\langle \Delta n_0 \rangle \simeq \frac{dn}{dT} \frac{\alpha F}{2\rho C_v} , \tag{17}$$

where ρ is the density, C_v is the specific heat and dn/dT is the thermo-optic coefficient of the medium. The factor of 2 comes from the temporal averaging.[10] The coefficient dn/dT has long been investigated for CS_2, and a value of $\simeq -8 \times 10^{-4}$ °C^{-1} has been reported in the literature.[21] With the known value of $\rho C_v \simeq 1.3$ J/Kcm^3 for CS_2, we obtain $\langle \Delta n_0 \rangle \simeq 1.1 \times 10^{-3}$ at a $\simeq 17$ J/cm^2 fluence. This is in good agreement with the $\langle \Delta n_0 \rangle \simeq -1.0 \times 10^{-3}$ used to fit the Z-scan of Fig. 9. Note that in this calculation, a value of $\simeq 5$, as obtained for $S \simeq 0.5$, was used for the a parameter. Note also that the $z = 0$ point in the Z-scan curve is defined as the position of the focus in air in the absence of the nonlinear medium. After the insertion of a thick sample with $n_0 > 1$, the beam waist inside the sample no longer will coincide with our $z = 0$ point. This is why the $z = 0$ point of the Z-scan in Fig. 9 differs from that of Fig. 4, which was calculated assuming $n_0 = 1$.

The limiting behavior of the same CS_2 cell at 10.6 μm was shown in Fig. 2, where the normalized transmitted power was plotted versus the input power as measured for the various sample positions indicated in Fig. 9. They exhibit the predicted features given in Fig. 7. It is evident from Eq. (17) that thermal self-action can be enhanced by increasing the absorption coefficient of the medium. We obtained a limiting threshold of $\simeq 0.5$ kW (150 μJ) in CS_2 at 10.6 μm by desolving impurities (e.g., sulfur) to increase the absorption coefficient to $\simeq 2$ cm^{-1}. This is shown in Fig. 10 where the results for two samples of pure and modified

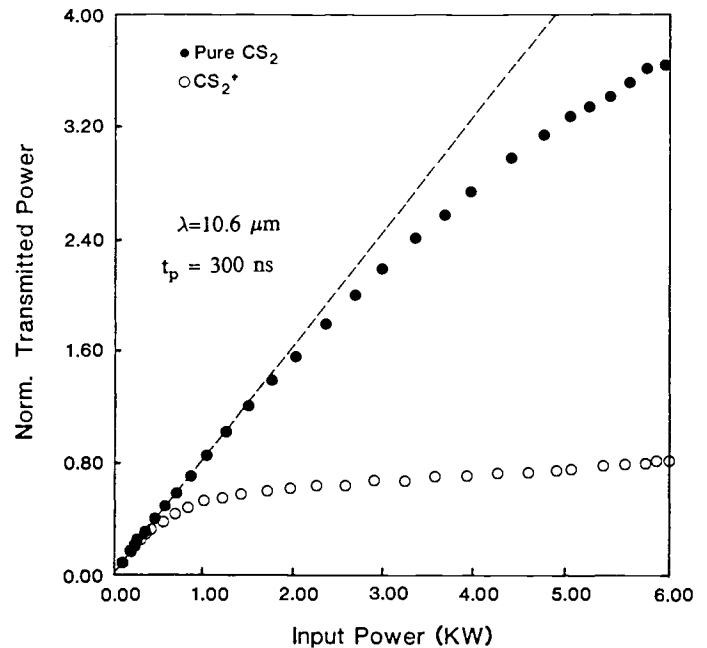Fig. 9. The measured Z-scan of a 24-mm thick CS_2 sample using 300-ns TEA CO_2 laser pulses at 10.6 μm. The theoretical fit (solid curve) is obtained based on thermal self-defocusing in CS_2. The arrows on the z-axis indicate the positions at which the limiting data of Fig. 2 were obtained. Because $n_0 \neq 1$, the curve is no longer symmetric about $z = 0$.

Fig. 10. A low-threshold fluence limiter at 10.6 μm using modified CS_2 ($\alpha \simeq 2$ cm^{-1}) as compared to pure CS_2 ($\alpha \simeq 0.22$ cm^{-1}). The measurements were obtained using a 3-mm cell placed at the transmittance valley.

CS_2 are compared for a 3-mm cell positioned in the transmittance valley.

Liquid CS_2 is also well known for its strong optical Kerr effect with a relatively dispersionless nonlinear index $\gamma \simeq +3 \cdot 4 \times 10^{-14}$ cm^2/W ($n_2 \simeq 1.3 \times 10^{-11}$ esu).[22-24] This effect was ignored when the thermal nonlinearity was dominant as was the case with 30-ns pulses. With picosecond pulses, however, $t_p \ll t_{ac}$ and nonlocal nonlinearities such as thermal or electrostriction no longer dominate. Thus, the reorientational Kerr effect with $\simeq 2$ picosecond decay time[22] becomes the dominant mechanism for nonlinear refraction. Using 130-ps "optical free-induction decay" pulses at 10.6 μm (Ref. 25) and a peak power of 350 kW, we performed Z-scans with the 24-mm CS_2 cell. The result as shown in Fig. 11 exhibits a valley-peak configuration showing self-focusing indicative of the positive sign of the Kerr coefficient. The theoretical fit in Fig. 11 with $S = 0.4$ is obtained using $n_2 \simeq 1.5 \times 10^{-11}$ esu, which is in close agreement with previously reported values of n_2 in CS_2 measured in the visible and near IR regions.[23,24] Note that use of gentler focusing gives a larger diffractive length ($z_0 = 4$ mm or $l = 3.7$), resulting in the disappearance of the rather flat portion of the Z-scan that was more visible in Fig. 9.

A quick estimate of the nonlinear phase shifts can be evaluated from Eq. (15) and L_{eff} as obtained from Fig. 6 for both nanosecond and picosecond Z-scan experiments.

6. CONCLUSION

We have shown that limiting in thick Kerr-like media may be simply modeled using a modification of the aberration-free approximation. For small nonlinear phase shifts ($\Theta < 2$), this model shows excellent agreement with our Z-scan and limiting experiments. Therefore, we conclude that the method is of considerable use both in experimental measurement of n_2 in thick media and in designing optimized limiting devices.

This extension of our ability to measure n_2 in media thicker than the depth of focus may find application for media where the nonlinearity is small and the laser beam must be focused very tightly to see a measurable effect. This is exemplified by our picosecond 10.6-μm measurement of n_2 in CS_2, shown in Fig. 11. Here, $l = 3.7$ so that $l_{eff} \simeq 1.5$, whereas if a truly thin sample were used, $l_{eff} \ll 1$. Given that the result shown in Fig. 11 was obtained with the maximum energy available from our picosecond source, a measurement of n_2 would not have been possible with a thin sample. Furthermore, we have shown that a quick estimate of the nonlinear coefficient can be deduced from the Z-scan transmittance curve of a thick media by using the calculated effective interaction length l_{eff}, introduced in Sec. 3.

The results of this modeling as applied to limiting indicate that the minimum limiting threshold is obtained by positioning the focus at the front (or rear) surface of the sample for a negative (or positive) nonlinearity, respectively. In both cases this corresponds to the Z-scan valley. Such a conclusion might lead one to believe that such limiters are inherently prone to damage, because a positive n_2 with a long propagation path leads to catastrophic beam collapse. Similarly, for a negative n_2, the beam must be focused on the damage-prone front surface. However, other geometries for limiting may be envisioned that do not have this problem. For example, the simple addition of a second lens behind the sample will reverse the order of peak and valley in some plane after the lens. Thus, for a negative n_2, the limiting is optimized with the focus at the rear surface.[26] Although to consider the optimization of other possible geometries is beyond the scope of this paper, the method of analysis introduced here should be adequate for such a task. However, the model has been applied to a purely refractive third-order nonlinearity in the presence of linear absorption. Nonlinear absorption, such as occurs in semiconductor limiters, has not yet been included.[3]

In light of the conclusions made here, the observations reported in the "Chinese Tea" paper[15] are easily understood as being due to simple thermal defocusing. The reported sign change of the nonlinearity was not in fact a sign change, but simply the consecutive observation of the transmission "valley" to "peak" as the sample position was changed with respect to focus.

7. APPENDIX

To examine the validity and limitations of the "constant shape" approximation, we compare Eq. (9) in the limit of the small phase distortion with that of Ref. 10, which was obtained using the Fresnel wave optics approach.

The far field condition imposed by having $D \gg 1$ (see Fig. 1) along with the small phase distortion assumption ($|\Delta\Phi_0| < 1$) will reduce Eq. 9 to

$$\frac{w_a^2}{w_0^2} \simeq D^2 \left(1 - \frac{4x\Delta\Phi_0/a}{(1 + x^2)^2}\right) .$$ (18)

The on-axis($S \simeq 0$) irradiance is then inversely proportional to the beam area ($\pi w_a^2/2$). Therefore, the normalized on-axis transmittance is simply obtained as

$$T(\Delta\Phi_0, x) \simeq 1 + \frac{\Delta\Phi_0}{a} \frac{4x}{(1 + x^2)^2} .$$ (19)

The extrema (peak and valley) of the transmittance can be obtained from $dT/dx = 0$. This gives $x_{p,v} = \pm 1/\sqrt{3}$ as compared to the more rigorous result of ± 0.858 as given in Ref. 10. The peak-valley transmittance difference can, therefore, be deduced as

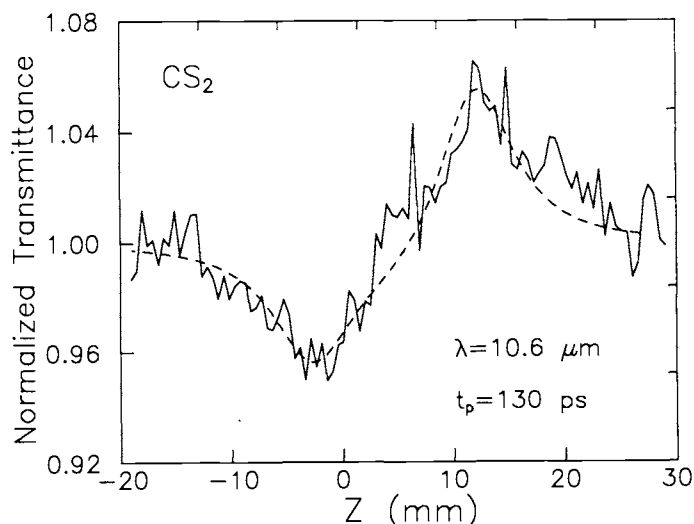$$\Delta T_{p-v} = T(\Delta\Phi_0, x_p) - T(\Delta\Phi_0, x_v) = p|\Delta\Phi_0| ,$$ (20)

Fig. 11. The measured Z-scan of the 24-mm CS_2 sample using 130-ps CO_2 laser pulses. The broken line is the calculated result using $n_2 = 1.5 \times 10^{-11}$ esu. Here $S = 0.4$ giving $a = 5.4$.

where $p = 3\sqrt{3}/(2a)$. Equating this value for p with the value of $p \simeq 0.406$ (Ref. 10) yields $a \simeq 6.4$, indicating the significance of introducing this correction factor into the aberration-free approximation theory.

8. ACKNOWLEDGMENTS

9. REFERENCES

1. R. C. C. Leite, S. P. Porto, and T. C. Damen, "The thermal lens effect as a power-limiting device," *Appl. Phys. Lett.* 10, 100–101 (1967).
2. W. E. Williams, M. J. Soileau, and E. W. Van Stryland, "Optical switching and n_2 measurements in CS_2," *Opt. Commun.* 50, 256–260 (1984).
3. E. W. Van Stryland, Y. Y. Wu, D. J. Hagan, M. J. Soileau, and K. Mansour, "Optical limiting with semiconductors," *J. Opt. Soc. Am.* 5, 1980–1989 (1988).
4. J. H. Hermann, "Simple model for a passive optical power limiter," *Opt. Acta* 32, 541–547 (1985).
5. A. E. Kaplan, "External self-focusing of light by a nonlinear layer," *Radiophys. Quantum Electron.* 12, 692–696 (1969).
6. E. W. Van Stryland, H. Vanherzeele, M. A. Woodall, M. J. Soileau, A. L. Smirl, S. Guha, T. G. Boggess, "Two-photon absorption, nonlinear refraction, and optical limiting in semiconductors," *Opt. Eng.* 25, 613–623 (1985).
7. J. R. Hill, G. Parry, and A. Miller, "Nonlinear refraction index changes in CdHgTe at 175 k with 1.06 μm radiation," *Opt. Commun.* 43, 151–156 (1982).
8. T. F. Boggess, S. C. Moss, I. W. Boyd, and A. L. Smirl, "Picosecond nonlinear-optical limiting in silicon," in *Ultrafast Phenomena IV*, D. H. Huston and K. B. Eisenthal, eds., Springer-Verlag, New York, pp. 202 (1984).
9. M. Sheik-Bahae, A. A. Said, and E. W. Van Stryland, "High sensitivity, single beam n_2 measurements," *Opt. Lett.* 14, 955–957 (1989).
10. M. Sheik-Bahae, A. A. Said, T. H. Wei, D. J. Hagan, and E. W. Van Stryland, "Sensitive measurement of optical nonlinearities using a single beam," *IEEE J. Quantum Electron.* 26, 760–769 (1990).
11. M. Sheik-Bahae, A. A. Said, D. J. Hagan, M. J. Soileau, and E. W. Van Stryland, "Simple analysis and geometric optimization of passive optical limiters based on internal self-action," in *Materials for Optical Switches and Limiters*, Proc. SPIE 1105, 146–153 (1989).
12. D. J. Hagan, E. W. Van Stryland, M. J. Soileau, Y. Y. Wu, and S. Guha, "Self-protecting semiconductor optical limiters," *Opt. Lett.* 13, 315–317 (1988).
13. S A. Akhmanov, A. D. Sukhorokov, and R. V. Khokhlov, "Self-focusing and diffraction of light in a nonlinear medium," *Sov. Phys. Usp.* 10, 609 (1968).
14. A. Yariv and P. Yeh, "The application of Gaussian beam formalism to optical propagation in nonlinear media," *Opt. Commun.* 27, 295–298 (1978).
15. H. J. Zhang, J. H. Dai, P. Y. Wang, and L. A. Wu, "Self-focusing and self-trapping in new types of Kerr media with large nonlinearities," *Opt. Lett.* 14, 695–696 (1989).
16. G. M. Zverev and V. A. Pashkov, "Self-focusing and laser radiation in solid dielectrics," *Sov. Phys. JETP* 30, 616 (1970).
17. M. J. Soileau, W. E. Williams, N. Mansour, and E. W. Van Stryland, "Laser-induced damage and the role of self-focusing," *Opt. Eng.* 28, 1133–1144 (1990).
18. J. H. Marburger, "Progress in quantum electronics," J. H. Sanders and S. Stenholm, eds., Pergamon, New York, p. 35 (1977).
19. M. D. Feit and J. A. Fleck, Jr., "Beam nonparaxiality, filament formation, and beam breakup in the self-focusing of optical beams," *J. Opt. Soc. Am. B* 5, 633–640 (1988).
20. J. N. Hayes, "Thermal blooming of laser beams in fluids," *Appl. Opt.* 2, 455–461 (1972).
21. V. Raman and K. S. Venkataraman, "Determination of the adiabatic piezo-optic coefficient of liquids," *Proc. R. Soc. London A.* 171, 137 (1939).
22. P. P. Ho and R. R. Alfano, "Optical Kerr effects in liquids," *Phys. Rev. A* 20, 2170–2187 (1979).
23. I. Golub, Y. Beaudoin, and S. L. Chin, "Nonlinear refractions in CS_2 at 10.6 μm," *Opt. Lett.* 13, 488–491 (1988).
24. P. Thomas, A. Jares, and B. P. Stoicheff, "Nonlinear refractive index and "DC" Kerr constant of liquid CS_2 at 10.6 μm," *IEEE J. Quantum Electron.* QE-10, 493–494 (1974).
25. M. Sheik-Bahae and H. S. Kwok, "Characterizations of a picosecond CO_2 laser system," *Appl. Opt.* 24, 666–670 (1985).
26. J. A. Hermann and P. B. Chapple, "External self-focusing and in a two-lens system: shift and compression of the focal profile," Submitted to *J. Mod. Opt.*